RSC Advances

REVIEW

View Article Online
View Journal | View Issue

Cite this: *RSC Adv.*, 2025, **15**, 43013

Imide-based covalent organic frameworks: molecular design, synthesis, and applications in clean energy and environmental remediation

Premchand Panda [b] and Tamas Panda *[a]

Received 9th August 2025
Accepted 23rd October 2025

DOI: 10.1039/d5ra05831g

rsc.li/rsc-advances

Imide-based covalent organic frameworks (Imide-COFs) have emerged as a chemically robust subclass of COFs, distinguished by their π-conjugated backbones, high crystallinity, and structural tunability. This class of COF constructed *via* condensation reactions between electron-deficient aromatic dianhydrides and electron-rich diamines, these frameworks exhibit strong donor–acceptor interactions that impart intrinsic redox activity and facilitate efficient charge transport. Such properties make Imide-COFs attractive candidates for applications in electrochemical energy storage, photocatalysis, and clean energy conversion. Their extended π-systems and accessible pore networks further support guest–host interactions relevant to gas adsorption, ion transport, and environmental remediation. This review highlights recent advances in the rational design and synthesis of Imide-COFs, correlating their molecular structures with functional performance in energy-related applications such as lithium/sodium-ion batteries, supercapacitors, and water-splitting systems. We also discuss their potential in pollutant removal and other environmental technologies, and conclude with a perspective on future opportunities for developing Imide-COFs as multifunctional materials for sustainable energy and environmental solutions.

1 Introduction

The pursuit of advanced materials for sustainable energy storage and environmental remediation continues to be a central focus in materials chemistry. Researchers are increasingly drawn to porous materials due to their tunable structures, high surface areas, and capacity to host chemical functionalities relevant for gas adsorption, separation, catalysis, and pollutant removal.[1] A wide range of porous materials has been developed to date, including cross-linked polymers,[2] conjugated porous polymers,[3–5] organic porous networks,[6] and coordination frameworks such as metal–organic frameworks (MOFs)[7] and covalent organic frameworks (COFs).[7] Among these, COFs stand out as a unique class of crystalline porous polymers formed by the reticular assembly of organic building blocks through strong covalent bonds into periodic, porous architectures.[8]

Since the pioneering report of the boroxine-linked COF by Yaghi *et al.*,[9] the field has rapidly expanded, with new synthetic strategies and linker chemistries enabling the construction of COFs with diverse topologies, functionalities, and properties. The formation of COFs typically relies on reversible condensation reactions, allowing dynamic covalent chemistry to facilitate error correction during framework crystallization. Structural rigidity, planarity, and symmetric connectivity of monomers are essential to generate long-range ordered frameworks and to suppress the formation of amorphous networks.[10] Over the years, various linkages—including boronate esters, imines, triazines, hydrazones, β-ketoenamines, and imides—have been explored to tailor COF properties for targeted applications.[11]

Among the diverse linkage chemistries, imide linkages (–C(=O)–N–C(=O)–) have attracted increasing attention due to their inherent chemical and thermal robustness. It follows the mechanism in which a polycondensation reaction happens between amine and anhydride at high temperatures. Studies in the literature indicate 1st imide-based COFs was reported in 2014.[12] Imide-COF crosslinking is formed by the active sites present in the starting materials. The Imide-COF material property depends upon the rigidity and flexibility of the monomer. The intermolecular or intramolecular charge transfer results in the colour, photoconductivity, and electroconductivity of Imide-COFs. The electron acceptor and donor monomer results the COF skeleton redox active, makes suitable for electro catalytic applications. The imide groups are highly polar, which enhance the attraction towards CO_2, SO_2, *etc* through dipole–quadrupole interactions.[13] Highly crosslinked Imide-COFs offer numerous advantages due to their exceptional physical and chemical properties. They have a wide range of potential applications because of their exceptional features, including adsorption and separation of gases, energy storage,

[a]*Centre for Clean Environment, Vellore Institute of Technology, Vellore, Tamil Nadu 632014, India. E-mail: tamaskumarpanda@vit.ac.in*

[b]*Department of Chemistry, School of Advanced Sciences, Vellore Institute of Technology, Vellore, Tamil Nadu 632014, India*

heterogeneous catalysis, delivery of drugs, and the removal of heavy metals from water.[14]

While previous reviews have introduced the chemistry and potential of imide-based COFs, a comprehensive account that links their molecular design and synthetic strategies to their roles in energy and environmental technologies remains limited. In this review, we systematically highlight recent developments in the synthesis and structural engineering of Imide-COFs, with a focus on their emerging applications in clean energy conversion, electrochemical storage, and environmental remediation. To the best of our knowledge, this is the first focused review that consolidates the progress of Imide-COFs from inception to current state-of-the-art, with an emphasis on their contribution to energy sustainability and environmental stewardship.

2 Mechanism and design principle of imide-based COFs

2.1 Mechanism

To realize the potential of imide-based COFs in energy and environmental applications, a deep understanding of their underlying chemistry and synthetic methodologies is essential. Central to the formation of imide linkages is the imidization reaction, a well-established transformation in polymer chemistry. In general, the reaction between an aromatic amine and an aromatic dianhydride in a dipolar aprotic solvent such as, *N*-methyl-2-pyrrolidone (NMP) and catalyst quinoline leads to the formation of an imide-based linkage. This process typically proceeds *via* an intermediate poly (amic acid), which undergoes intramolecular cyclodehydration to yield the thermally and chemically stable imide bond. Mechanistically, the reaction begins with the nucleophile attack on the carbon atom of the carbonyl carbon of the anhydride ring, followed by ring opening and the formation of a poly(amic acid) intermediate. Subsequent dehydration facilitates cyclization and imide ring formation, completing the imidization process (Fig. 1a).[15]

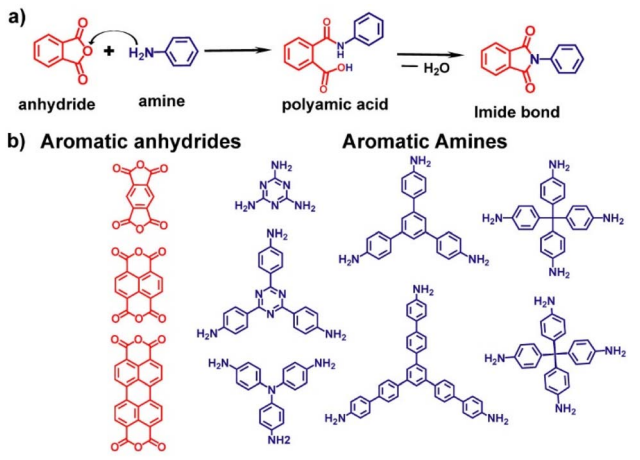

Fig. 1 (a) Schematic representation for the synthesis of imide bond formation. (b) List of aromatic anhydrides and aromatic amines employed for the preparation of imide-COFs. All the structures were drawn in Chemdraw software.

3 Design principle

The architectural design of COFs primarily depends on the geometry of the building blocks. Typically, the synthesis of 1D COFs involves the combination of one four-linked ligand with a V-shaped C_2-symmetric ligand. These 1D chains are stacked together through π–π interactions, van der Waals forces, and hydrogen bonding. Following this design principle, Li *et al.* (2024) reported the first 1D imide COFs, namely NiPc-CZDM-COF and NiPc-CZDL-COF. Reports on 1D imide COFs remain limited due to the scarcity of suitable linkers, whereas a considerable number of 2D imide COFs have been successfully synthesized. The synthesis of 2D COFs generally employs C_2-, C_3-, or C_4-symmetric aromatic linkers. In the case of 2D imide COFs, a $C_2/C_3/C_4$-symmetric aromatic amine linker is typically coupled with a C_2/C_3-symmetric aromatic anhydride or dicarboxylic linker. The combination of linkers with different symmetries results in COFs with distinct topologies—such as hexagonal (C_3 + C_2), square (C_4 + C_2), or star-shaped (C_4 + C_2) frameworks. Although 2D imide COFs have been extensively explored, reports on 3D imide COFs are rare. The synthesis of 3D imide COFs usually involves Td-symmetric aromatic amines combined with C_2/C_4-symmetric aromatic anhydride linkers. This structural diversity and the presence of varied functional groups within imide COFs contribute to their potential applications in energy storage and environmental remediation.

A variety of synthetic methodologies have been employed to construct imide-COFs with high crystallinity and porosity. These include conventional condensation polymerization,[17] solvothermal synthesis,[12] hydrothermal methods,[18] high-temperature solid-state synthesis,[19] ionothermal routes,[20] and ionic liquid-assisted strategies[21] (Table 1). The choice of method significantly influences the crystallinity, surface area, and morphological features of the resulting COFs.

In the following sections, we first discuss in detail the various synthesis strategies and critical parameters that govern the successful formation of imide-COFs. This is followed by an in-depth examination of their functional applications, particularly in sustainable energy storage/conversion and environmental remediation.

3.1 Synthesis strategies of imide-based COFs

A diverse range of synthetic strategies has been developed to construct imide-based COFs with tailored properties for energy and environmental applications. These methodologies include solvothermal, condensation polymerization, hydrothermal, ionothermal, ionic liquid-assisted, and high-temperature solid-state techniques. Each approach offers distinct advantages in terms of crystallinity, scalability, environmental safety, and control over pore structure and surface area. The choice of synthesis method is closely tied to the physicochemical characteristics of the selected monomers, their symmetry, and reactivity, as well as the targeted application of the final framework.

Table 1 Different types of imide-COFs, their synthesis procedure, and applications

Synthesis procedure	COFs	Applications	S_{BET} (m^2 g^{-1})	References
Solvothermal synthesis				
	PI-COF-1, PI-COF-2, PI-COF-3	RhB dye adsorption	1027, 1297, 2346	12
	PI-COF-4, PI-COF-5	Drug delivery	2403, 1876	25
	PI-CONs	2, 4,6-TNP sensing	894	37
	PIBN-G	Li^+ ion battery	350	38
	PAF-110	Acetylene adsorption	910	39
	MIT-COF-1, MIT-COF-2	CO_2 absorption	339, 397	26
	NDI-COF	ORR catalysis	1138	31
	PI-NT-COF	Memory device		40
	TP-COF	Li^+ ion battery	960	41
	PMDA-TAPB	Fe^{3+}, Pb^{2+}sensing	1194.4	42
	HATN-AQ-COF	Li^+ ion battery	725	27
	2D-PT-COF, 2D-NT-COF	Aluminium battery	1118,1083	43
	PI-COF	Zn^{2+} ion battery		44
	TAPA-NDI-COF, TAPB-NDI-COF, TAPT-NDI-COF	ORR catalysis	1283, 1138,501	32
	Cryst-2D-PMPI	HER catalysis	18	34
	PI-COF-1, PI-COF-2, PI-COF-TT	CO_2 photo catalytic reduction reaction	475,1175,825	35
	TPPICOF	Uranium adsorption	1998.5	61
	PIT COF	Li^+ ion battery	674	62
	COF-JLU-85, COF-JLU-86	Li^+ ion battery	215,491	63
	PT-COF, PB-COF	H_2O_2 photosynthesis	782,844	64
	TAPA-PDI-COF	Solid state Li+ electrolyte	91	65
	PIQ-COF	Aqueous proton battery	55.3	66
	MTI-DAPy-COF	Proton conducting material	207.9	67
Condensation reaction				
	NT-COF	Solar to electrochemical energy storage	1276	17
	NDI-*N*-COF, NDI-B-COF	ORR catalyst	1119, 1025	22
	PI-COF	Solar cell		45
Hydrothermal synthesis				
	PIC-Ph, PIC-Dp	Li^+ ion battery	669, 125	18
	HATN-PD-COF, HATN-TAB-COF	Na^+ ion battery	1200, 1065	60
Ionothermal synthesis				
	TAPB-PTCDA, TAPB-PMDA	Green synthesis	460, 1250	20
Ionic liquid-assisted synthesis				
	PMDA-TAPA	CO_2 adsorption	35.4	21
High temp. solid state synthesis				
	PI-COF-201, PI-COF-202	Fe^{3+} sensing	3.929, 9.161	19
	COF-1, COF-2	Fe^{3+} sensing		30
	PIA, PIB, PIC, PID	CO_2 adsorption Na^+ ion battery	580, 760, 990, 1430	46
	Be–PICOF, Na–PICOF, Pe–PICOF	Li^+ ion battery		47
	PCOFs	Heterogenous catalysis	36.36	48
	MAB1	N_2/O_2 separation	3.28	49

3.2 Solvothermal synthesis

Solvothermal synthesis remains one of the most established and widely utilized methods for constructing imide-based COFs with high crystallinity and well-defined porous structures. This approach typically involves the reaction of aromatic amines with aromatic dianhydrides in high-boiling-point solvents, such as mesitylene and 1,4-dioxane, in the presence of a base catalyst like isoquinoline. The reaction mixture is sealed in high-pressure-resistant Pyrex or autoclave tubes and heated at elevated temperatures (150–200 °C) for 3–5 days.[23] The success of this method depends strongly on the reversibility of the imidization reaction and the solubility and reactivity of the chosen monomers.

In 2014, Tian, Dan, *et al.* reported an amorphous polyimide network synthesized from pyromellitic dianhydride (PMDA) and 1,3,5-tris(4-aminophenyl)benzene (TAPB).[24] Interestingly, in the same year, Yan and co-workers achieved the first crystalline imide-linked COFs *via* solvothermal polymerization of PMDA with three different C_3-symmetric aromatic amine linkers: tris(4-aminophenyl)amine (TAPA), TAPB, and 1,3,5-tris

[4-amino(1,1-biphenyl-4-yl)]benzene (TABPB). The resulting frameworks—PI-COF-1, PI-COF-2, and PI-COF-3—were synthesized in a mesitylene/dioxane mixture (1 : 1 v/v) using isoquinoline as a base catalyst at 200 °C over five days.[24] The role of the catalyst is crucial for controlling the rate of polyimidization, while the high reaction temperature facilitates the ring-closing cyclization and enhances the overall crystallinity of the COFs. Building on this strategy, the same group reported two additional crystalline frameworks, PI-COF-4 and PI-COF-5, in 2015.[25] These 3D COFs were synthesized using tetrahedral amine linkers such as 1,3,5,7-tetraaminoadamantane (TTA) and tetra(4-aminophenyl) methane (TAPM), combined with PMDA as the anhydride linker. Both frameworks displayed diamond-like topologies and retained good crystallinity, as confirmed by PXRD analysis. Between 2014 and 2019, a series of di-imide-based COFs were synthesized using similar solvothermal strategies, with varied linker combinations to tune pore size, dimensionality, and surface area (Table 1). In 2019, Veldhuizen and co-workers extended this chemistry to tri-imide systems, synthesizing MIT-COF-1 and MIT-COF-2 *via* condensation of mellitic trianhydride (MTA) with TAPB and TAPA, respectively.[26] These tri-functional linkers enabled denser cross-linking and potentially improved framework stability. More recently, in 2022, Jiang *et al.* introduced HATN-AQ-COF, a novel tri-imide-based COF synthesized *via* the solvothermal reaction of 2,3,8,9,14,15-hexacarboxy-hexazatrinaphthalene trianhydride (HATN-AP) with 2,6-diaminoanthraquinone (DAAQ).[27] This framework exhibited sharp and intense PXRD peaks ($2\theta = 2.22°$, 3.86°, 5.94°), indicating superior crystallinity relative to previously reported polyimide COFs (Fig. 2f). Notably, HATN-AQ-COF represents the first tri-imide mesoporous COF with a large pore size of 3.8 nm and a high Brunauer–Emmett–Teller (BET) surface area of 725 $m^2\ g^{-1}$ (Fig. 2b), making it a promising candidate for applications requiring high porosity and structural order.

3.3 Condensation polymerization synthesis

In contrast to the solvothermal approach, the synthesis of imide-based COFs *via* condensation polymerization does not require sealed tubes or high-pressure setups. Instead, this method utilizes a conventional reflux or heating setup under inert or dry conditions, making it operationally simpler and more scalable. The first successful application of this method for crystalline imide-COF synthesis was reported by Wang and co-workers in 2018.[17] They employed a linear aromatic anhydride linker, 1,4,5,8-naphthalene tetracarboxylic dianhydride (NTDA), in combination with the C_3-symmetric amine linker tris(4-aminophenyl) amine (TAPA), in dry *N*, *N*-dimethylformamide (DMF). The reaction mixture was heated at 180 °C for 3 days, leading to the formation of a crystalline imide-linked COF, termed NT-COF. Structural analysis revealed that NT-COF adopts a bnn topology and possesses a high Brunauer–Emmett–Teller (BET) surface area of 1276 $m^2\ g^{-1}$, indicating excellent porosity and well-defined framework architecture. More recently, in 2022, Huang *et al.* expanded this strategy to synthesize two additional imide-linked COFs using condensation polymerization.[22] In their work, 1,4,5,8-naphthalene

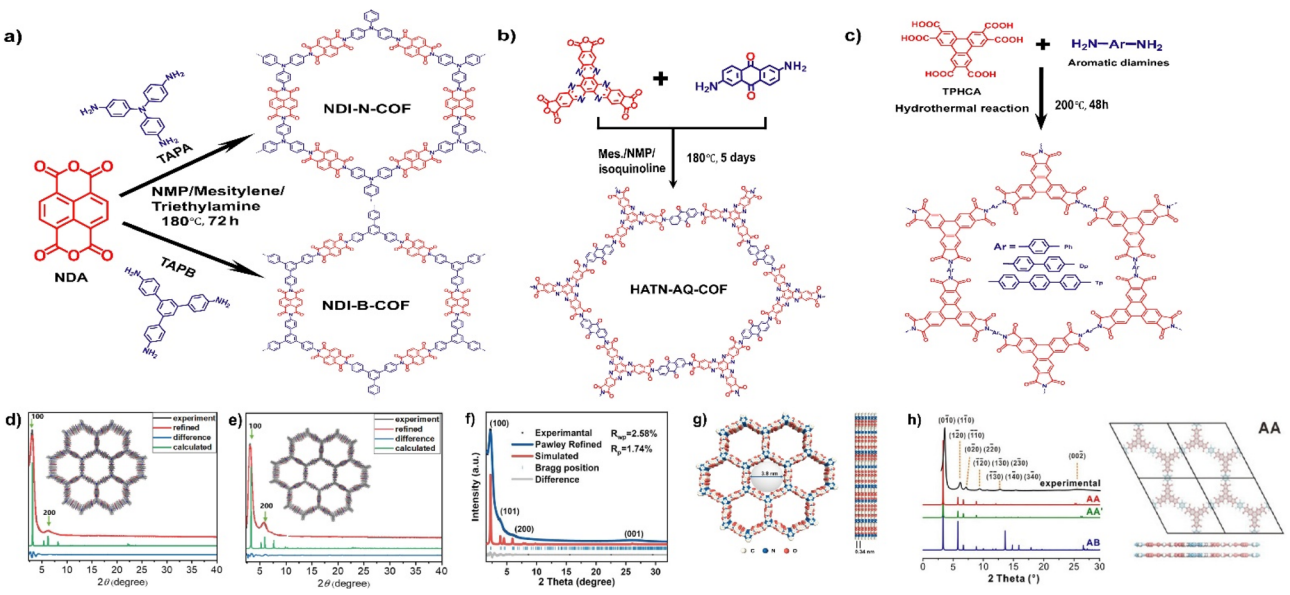

Fig. 2 (a) Schematic representation for the synthesis of NDI-*N*-COF, NDI-B-COF by condensation polymerization method. (b) Representation of the synthesis of HATN-AQ-COF by solvothermal synthesis method, (c) Hydrothermal synthesis method of 3D-PI-COFs. Powder X ray diffraction pattern of (d) NDI-*N*-COF and (e) NDI-B-COFs and (f) HATN-AQ-COF, compared with their corresponding simulated powder pattern. (g) Two-dimensional crystal structure of HATN-AQ-COF with AA stacking. (h) Experimental PXRD pattern compared with AA, AA′ and AB stacking simulated structure of PIC-Ph COF. Also, the AA stacking structure represented. Figure (a, d, and e) have been reproduced and adopted from reference no. 22 with permission from Elsevier, copyright 2022. Figure (b, f, and g) have been reproduced and adopted from reference no. 27 with permission from Wiley, copyright 2022. Figure (c, and h) have been reproduced and adopted from reference no. 18 with permission from Wiley, copyright 2021.

tetracarboxylic dianhydride (NTDA) was individually reacted with 1,3,5-tris(4-aminophenyl) benzene (TAPB) and tris(4-aminophenyl) amine (TAPA) to yield two highly crystalline frameworks, designated NDI-B and NDI-N, respectively (Fig. 2a). Both frameworks exhibited well-defined crystallinity and significant porosity, as confirmed by PXRD and nitrogen adsorption–desorption measurements (Fig. 2e and f). This condensation polymerization approach, with its relatively mild synthetic requirements and ability to produce high-quality frameworks, holds considerable promise for the scalable fabrication of imide-based COFs.

3.4 Hydrothermal synthesis

Following the success of condensation polymerization strategies, hydrothermal synthesis has emerged as another effective route for constructing imide-linked COFs. While conceptually similar to solvothermal synthesis, the hydrothermal approach uniquely employs water as the reaction medium instead of organic solvents. Under elevated temperature and pressure conditions, water undergoes significant changes in its physical and chemical properties—such as reduced hydrogen bonding, decreased viscosity, and altered dielectric constant—which collectively enhance the kinetics and diffusion-controlled nature of organic transformations. Additionally, the ionic product of water increases with temperature, promoting *in situ* acid- or base-catalyzed condensation reactions crucial for imide bond formation.

Leveraging these advantages, Kim *et al.* reported the first series of crystalline imide-COFs synthesized under hydrothermal conditions.[18] Using triphenylene-2,3,6,7,10,11-hexacarboxylic acid (TPHCA) as a C_3-symmetric polycarboxylic acid linker and three different diamine building blocks—*p*-phenylenediamine (Ph), 4,4′-diaminobiphenyl (Dp), and 4,4′-diamino-*p*-terphenyl (Tp)—they obtained three distinct polyimide COFs: PIC-Ph, PIC-Dp, and PIC-Tp (Fig. 2c). Among them, PIC-Ph exhibited the highest crystallinity, as evidenced by its well-defined PXRD peaks at $2\theta = 3.60°$, 6.16°, 7.18°, 9.36°, 12.76°, and 25.38°, corresponding to multiple (hkl) planes due to a slightly tilted layer stacking. In contrast, PIC-Dp displayed fewer diffraction planes, indicating lower order (Fig. 2h). BET analysis revealed that PIC-Ph also showed the highest surface area (669 $m^2\ g^{-1}$), while PIC-Dp and PIC-Tp exhibited significantly reduced porosity (125 $m^2\ g^{-1}$ and 54 $m^2\ g^{-1}$, respectively). This decrease in porosity is likely attributed to the increased number of phenyl rings in the Dp and Tp linkers, which reduce interlayer spacing and restrict pore volume. More recently, in 2024, two new triimide-based COFs—HATN-PD and HATN-TAB—were synthesized *via* hydrothermal methods using hexaazatrinaphthylenehexacarboxylic acid (HATNCA) as the anhydride precursor.[28] This linker was reacted with *p*-phenylenediamine (PD) and 1,3,5-tris(4-aminophenyl) benzene (TAB), respectively, to yield crystalline frameworks featuring C=O and C=N functional groups and tunable pore channels. These structural characteristics facilitated efficient Na^+ ion storage, highlighting the potential of hydrothermally synthesized imide-COFs in sodium-ion battery applications.

3.5 Ionothermal synthesis

While hydrothermal and solvothermal methods have proven effective for synthesizing imide-linked COFs, they often rely on high-boiling-point organic solvents such as mesitylene, 1,4-dioxane, or *N*, *N*-dimethylformamide. These solvents not only raise environmental concerns but also prolong reaction times. To address these limitations and promote a more sustainable synthesis pathway, ionothermal synthesis has emerged as a promising solvent-free alternative. Ionothermal synthesis leverages molten metal salts as both solvent and structure-directing agents under high-temperature conditions. This strategy enables efficient polymerization while eliminating the need for toxic organic media. In a pioneering report, Lotsch and co-workers demonstrated the successful synthesis of two imide-based COFs—TAPB-PMDA and TAPB-PTCDA—using zinc chloride ($ZnCl_2$) as the reaction medium.[20] The condensation of 2,4,6-tris(4-aminophenyl)benzene (TAPB) with pyromellitic dianhydride (PMDA) or perylene-3,4,9,10-tetracarboxylic dianhydride (PTCDA) was conducted at 300 °C for 48 hours in the absence of any organic solvent (Fig. 3a). Both TAPB-PMDA and TAPB-PTCDA COFs exhibited high crystallinity and porosity, as confirmed by PXRD and nitrogen sorption analyses (Fig. 3d and e). The ionothermal approach significantly reduces the reaction time and circumvents the need for soluble organic monomers, making it an attractive method for scalable and greener COF production. Collectively, solvothermal, hydrothermal, condensation polymerization, and ionothermal routes offer diverse platforms for constructing imide-linked COFs with tuneable properties. Each method brings unique advantages in terms of crystallinity, porosity, reaction conditions, and environmental impact, thereby broadening the design landscape for COFs aimed for further applications.

3.6 Ionic liquid-assisted synthesis

Building on solvent-free and environmentally conscious strategies like ionothermal synthesis, the use of ionic liquids (ILs) has emerged as another green and efficient approach for constructing imide-based COFs. Ionic liquids are salts composed entirely of ions that exhibit melting points below 100 °C. Due to their unique physicochemical properties—such as negligible vapor pressure, high thermal stability, and excellent solvating ability—ILs have gained widespread attention in catalysis, synthesis, and materials processing. Importantly, ILs are often considered environmentally benign because they are non-volatile, recyclable, and can function simultaneously as solvents and catalysts. Widely studied ILs such as, 1-butyl-3-methylimidazolium bis(trifluoromethylsulfonyl)imide ([BMIm][NTf_2]) and 1-(4-sulfobutyl)-3-methylimidazolium hydrogen sulfate ([BSMIm][HSO_4]) have been employed successfully in various organic transformations.[29] In a pioneering study in 2020, Zhao and co-workers demonstrated the first ionic liquid-mediated synthesis of imide-linked COFs.[21] Using 1-butyl-3-methylimidazolium hydrogen sulfate ([BMIm][HSO_4]) as the solvent, they carried out the polycondensation of pyromellitic dianhydride (PMDA) with amine linkers such as tris(4-aminophenyl)amine (TAPA) and 1,3,5-tris(4-aminophenyl)

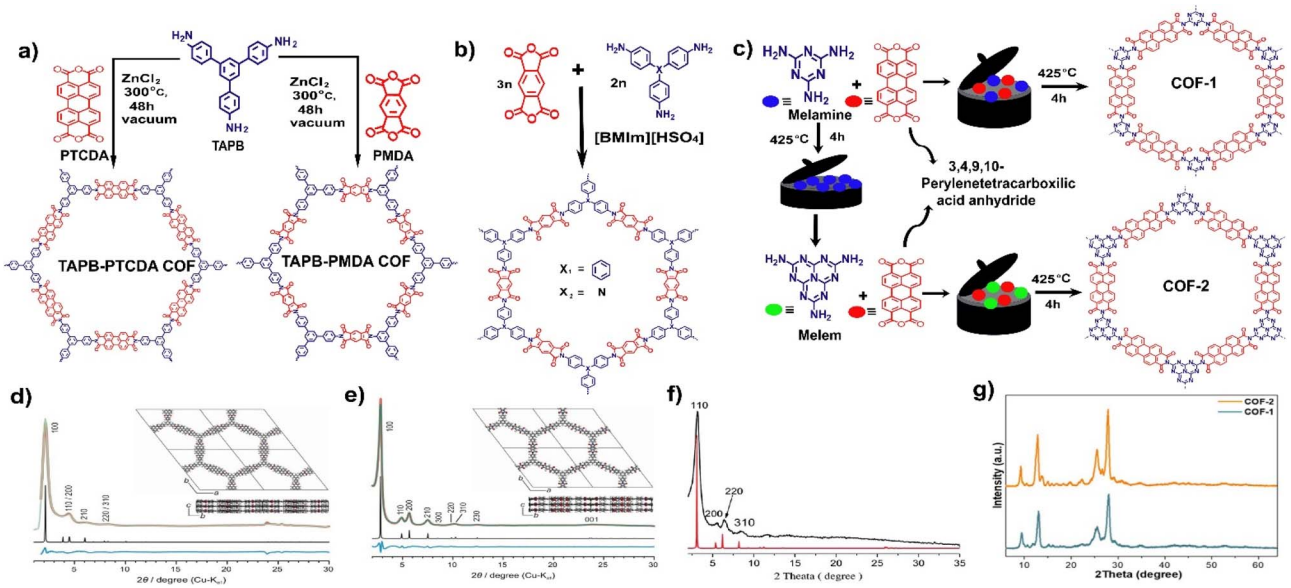

Fig. 3 (a) Ionothermal synthesis procedure of TAPB-PTCDA-COF and TAPB-PMDA-COF. (b) Ionic liquid assisted synthesis procedure of PMDA-TAPA-COF. (c) High temperature solid state synthesis of COF-1, COF-2, (d) Experimental PXRD patten of TAPB-PTCDA-COF, (e) PXRD of TAPB-PMDA-COF, (f) PMDA-TAPA COF and (g) COF-1 and COF-2, compared with their corresponding simulated powder X-ray diffraction pattern. Figure (a, d, and e) have been reproduced and adopted from reference no. 20. Figure (b and f) have been reproduced and adopted from reference no. 21 with permission from RSC, copyright 2020. Figure (c, and g) have been reproduced and adopted from reference no. 30 with permission from ACS, copyright 2021.

benzene (TAPB) under mild conditions (120 °C for 3 days) without any hazardous organic solvents (Fig. 3b and f). The resulting imide-based COFs exhibited good crystallinity and structural integrity. This ionic liquid-assisted approach not only avoids the use of toxic and volatile solvents but also offers improved control over reaction parameters such as temperature, solubility, and diffusion. Moreover, the recyclability of ILs enhances the sustainability of the process, aligning well with the principles of green chemistry. Together with solvothermal, hydrothermal, condensation polymerization, and ionothermal routes, ionic liquid-mediated synthesis expands the toolbox for constructing imide-linked COFs. These diverse synthetic strategies enable precise control over framework topology, porosity, and crystallinity—key factors that determine the performance of COFs in energy storage, separation, and environmental remediation applications.

3.7 High temperature solid state synthesis

Traditional solvothermal methods for synthesizing imide-based COFs typically involve the use of toxic organic solvents at elevated temperatures over prolonged durations, raising significant environmental and safety concerns. To address these issues, researchers have explored more sustainable, solvent-free synthetic approaches, among which high-temperature solid-state synthesis has emerged as a promising green strategy. In this method, organic monomers are heated beyond their melting points to facilitate direct condensation in the absence of any solvent. Upon melting, the monomers react to form oligomers, which then assemble into ordered COF structures through π–π stacking interactions. In 2017, Wu Yang and co-workers pioneered this approach by synthesizing two polyimide-linked COFs using melamine as the amine linker and two aromatic dianhydrides—pyromellitic dianhydride (PMDA) and naphthalene tetracarboxylic dianhydride (NTDA)—as the anhydride components. The solid-state reaction was conducted under nitrogen atmosphere at 325 °C for melamine–PMDA (yielding PI-COF-201) and at 345 °C for melamine–NTDA (yielding PI-COF-202), both in a 1 : 1 molar ratio.[19] Despite their relatively low surface areas (3.9 $m^2 g^{-1}$ and 9.2 $m^2 g^{-1}$, respectively), both frameworks exhibited high crystallinity and structural integrity. Later, in 2021, Shuo Wang's group introduced a modification to this protocol by incorporating a mechanochemical pre-activation step. Melamine and 3,4,9,10-perylenetetracarboxylic dianhydride were mixed and ground manually for 30 minutes at room temperature, followed by thermal treatment at 325 °C for 4 hours in ambient air, resulting in a crystalline framework referred to as COF-1 (Fig. 3c and g). A similar protocol was used to synthesize COF-2, where melem was used as the amine component instead of melamine.[30] This high-temperature solid-state synthesis offers several advantages, including elimination of hazardous solvents, shorter reaction times, and potential scalability, making it a valuable addition to the growing portfolio of green synthetic strategies for COF fabrication.

4 Characterization techniques for confirmation of imide COFs

Following the synthesis process, a series of advanced characterization techniques are employed to confirm the successful

formation of the desired imide-based COFs. These analyses not only validate the structural and compositional integrity of the synthesized frameworks but also provide critical insights into their frameworks but also provide critical insights into their morphological, textural, and functional properties.

4.1 Fourier transform infrared spectroscopy (FT-IR) analysis

The earliest reports of imide-based COFs appeared in 2014, attributed to Fang and co-workers, who utilized FT-IR spectroscopy to confirm the incorporation of imide functionalities within the COF backbone. For PI-COF-1, PI-COF-2, and PI-COF-3, distinct C–N–C stretching vibrations characteristic of the imide linkage were observed at 1375 cm^{-1}, 1371 cm^{-1}, and 1382 cm^{-1}, respectively. In a subsequent study, the same group synthesized two three-dimensional imide COFs named PI-COF-4 and PI-COF-5 which exhibited corresponding C–N–C stretching bands at 1336 cm^{-1} and 1353 cm^{-1}.[25] These findings indicate that the C–N–C vibrations associated with imide linkages generally appear within the 1350–1380 cm^{-1} range. Additionally, the asymmetric carbonyl stretching vibrations of imide groups typically occur between 1750 and 1780 cm^{-1}, while the symmetric carbonyl stretching bands are found in the 1700–1750 cm^{-1} region, further confirming successful imidization within the COF framework.

4.2 Powder X-ray diffraction (PXRD) analysis

Powder X-ray diffraction (PXRD) serves as a critical tool to determine whether COFs assemble into long-range ordered crystalline frameworks or exist merely as linear polymeric chains. Although numerous two-dimensional (2D) imide COFs have been reported, examples of one-dimensional (1D) and three-dimensional (3D) analogues remain limited due to inherent synthetic challenges. The first 1D imide COF was recently reported in 2024, synthesized using a V-shaped linker combined with a four-connected aromatic ligand. The resulting framework displayed characteristic diffraction peaks at 2θ = 4.51°, 7.62°, 11.73°, and 26.71°, corresponding to the (110), (310), (420), and (001) planes, respectively.[16] In contrast, the 3D imide COF (PI-COF-4)[25] exhibited distinct diffraction reflections at 2θ = 5.12°, 8.20°, 8.62°, 10.22°, 12.70°, 15.36°, 17.56°, and 18.94°, confirming the formation of a highly ordered three-dimensional extended framework.

4.3 Morphology analysis

Different synthetic approaches yield imide-based COFs with diverse morphological characteristics. Fang and co-workers were the first to synthesize PI-COF-1 to PI-COF-5 *via* a solvothermal method,[12,25] producing materials with predominantly spherical morphologies. More recently, in 2022, Kim and colleagues introduced a geomimetic hydrothermal approach, utilizing water as the reaction medium under elevated temperature and pressure to produce a series of polyimide COFs (PICs).[18] High-resolution TEM (HRTEM) analysis revealed that these hydrothermally synthesized PICs possessed fibrous morphologies with an average diameter of approximately 100 nm. Once the structural framework, crystallinity, and morphology of imide COFs are confirmed, their porosity can be further assessed using Brunauer–Emmett–Teller (BET) surface area analysis. The corresponding BET surface area values for the synthesized COFs are summarized in Table 1.

5 Applications of imide-based COFs

Building upon their robust synthesis routes and highly ordered structures, imide-based COFs have attracted significant attention for a broad range of applications. Their exceptional thermal and chemical stability, high surface area, and tailorable porosity combined with the presence of redox-active imide groups—render them highly suitable for energy and environmental technologies. Imide-COFs have emerged as promising candidates for clean and sustainable energy applications, including roles in electrocatalysis, photocatalysis, and energy storage devices such as batteries and supercapacitors. The carbonyl (C=O) groups inherent to the imide linkages serve as efficient coordination and electron-transfer sites, facilitating reactions central to electrocatalytic energy conversion, CO_2 reduction, and oxygen evolution. Additionally, their well-defined pore structures and functionalized channels enable selective interactions with gaseous and liquid pollutants, making them attractive materials for toxic gas adsorption, gas separation, and environmental remediation. These frameworks have also been successfully explored as heterogeneous catalysts, owing to their high thermal resistance and ability to incorporate metal or non-metal catalytic sites within their crystalline architecture. Overall, the multi-functionality of imide-based COFs, arising from both their structural robustness and chemical tunability, underscores their potential as next-generation materials for addressing global challenges in clean energy and environmental sustainability.

5.1 Electrocatalyst

According the demand for sustainable energy technologies is growing rapidly as global concerns over greenhouse gas emissions intensify. According to the U.S. Environmental Protection Agency, nearly 25% of global greenhouse gas emissions originate from the power generation sector, which still heavily relies on fossil fuels. To address this challenge, researchers have turned to renewable energy technologies such as fuel cells and water splitting systems that rely on oxygen reduction (ORR), oxygen evolution (OER), and hydrogen evolution reactions (HER). However, these processes typically require precious metal catalysts, such as platinum or its alloys, which are costly and scarce. Imide-based COFs have emerged as promising metal-free or metal-supported electrocatalysts, owing to their intrinsic redox activity, chemical robustness, and structurally tunable π-conjugated networks. Their porous frameworks ensure high surface area and efficient ion diffusion, which are crucial for enhancing electrocatalytic performance and improving the accessibility of active sites. Notably, naphthalene diimide (NDI)-based linkers have demonstrated significant potential for ORR catalysis, primarily due to the aromatic carbonyl groups and extended π–π conjugation that promote electron transfer. In 2020, Royuela

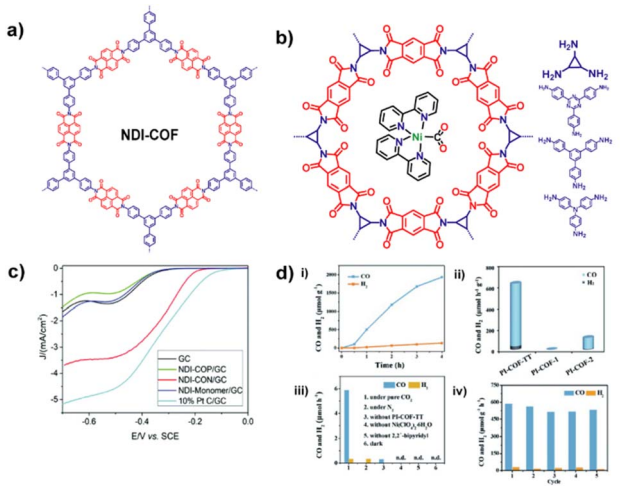

Fig. 4 (a) The structural representation of NDI-COF, (b) schematic representation of Ni composite doped inside the pore in the PI-COFs. (c) Electrochemical LSV plot of NDI-COFs, (d) (i) kinetic profile of CO production, (ii) catalytic performance of PI-COF, (iii) control experiments using PI-COF-TT, (iv) recycling test of PI-COF-TT. Figure (a, and c) have been reproduced and adopted from reference no. 31 with permission from RSC, copyright 2020. Figure (b, and d) have been reproduced and adopted from reference no. 35.

et al. reported the synthesis of an NDI-covalent organic network (NDI-CON) *via* the condensation of NTCDA and TAPB. The resulting material showed efficient ORR catalytic behavior with a low onset potential of −0.25 V *vs.* SCE under alkaline conditions (Fig. 4a and c).[31] Building on this, in 2022, Martínez-Fernández *et al.* synthesized three structurally distinct X-NDI-COFs by condensing naphthalene dianhydride (NDA) with different triamine linkers: TAPA, TAPB, and TAPT. These COFs exhibited good electrocatalytic activity toward ORR, each operating *via* a 4-electron transfer pathway. The observed overpotentials were −0.32 V for TAPB-NDI-COF and TAPT-NDI-COF, and −0.31 V for TAPA-NDI-COF, highlighting the influence of linker geometry on catalytic performance.[32] To further enhance catalytic activity, metal nanoparticles have been incorporated into COF architectures. In 2024, Zeng's group synthesized an imide-based COF from 4,4′,4″-(pyridine-2,4,6-triyl)trianiline (PTTA) and pyromellitic acid (PMA). Post-synthetic loading of Pd nanoparticles into the COF pores significantly boosted ORR performance, achieving a half-wave potential of 0.83 V *vs.* RHE.[33] Similarly, metal-doped COFs also exhibit remarkable electrocatalytic properties. In 2021, Pan *et al.* developed a ruthenium-doped NDI-based COF synthesized from melamine and PMDA, which displayed a notably low overpotential of 35.1 mV for HER, making it one of the most efficient COF-based electrocatalysts for hydrogen evolution.[34] These studies underscore the versatility and promise of imide-based COFs in advancing cost-effective, sustainable electrocatalysts for next-generation energy conversion technologies.

5.2 Photocatalyst

The porous and highly conjugated architecture of Imide-COFs facilitates efficient migration of photo-induced charges, thereby enhancing their potential in photo- and optoelectronic applications. Their well-defined pores not only allow for effective charge transport but also provide a versatile platform for heteroatom doping, which is essential for improving photocatalytic activity. In 2020, Chen, Xin *et al.* developed a photocatalytic system by incorporating Ni-based metal complexes into a series of PI-COFs, namely PI-COF-1, PI-COF-2, and PI-COF-TT, for the photoreduction of CO_2. Post-synthetically, a $[Ni(bpy)_3]^{2+}$ complex was introduced into the COFs to form Ni@PI-COF composites. Upon UV-vis irradiation, photogenerated electrons from PI-COF-TT reduced $[Ni(bpy)_3]^{2+}$ to the catalytically active $[Ni(bpy)_2]^0$ species. Meanwhile, CO_2 molecules interacted with various electron-rich units in the COF skeleton—such as tertiary amines, phenyl rings, triazine units, and imide moieties primarily through weak dipole–quadrupole interactions. Among these, the triazine units exhibited the strongest interaction due to their high electron density. As a result, PI-COF-TT achieved a CO production rate of 1933 μmol g^{-1} in 4 hours, significantly outperforming its counterparts. The study concluded that the synergistic contribution of the Ni centers and imide units in the COF backbone was key to the enhanced photocatalytic activity (Fig. 4b and d).[35] Designing COFs with both electron donor (D) and electron acceptor (A) functionalities is a promising strategy for boosting photocatalytic efficiency. Since imide groups serve as strong electron acceptors, introducing donor units (*e.g.*, metals or electron-rich linkers) can create D–A-type COFs, facilitating efficient charge separation. Building on this approach, researchers have also developed D–A–A systems, which further promote directional charge transfer *via* a push–pull–pull mechanism. For instance, a strong electron-accepting diamine linker, DNI-2NH_2 (2,7-bis(4-aminophenyl)-3a,5a,8a,10a-tetrahydrobenzo[lmn][3,8] phenanthroline-1,3,6,8(2H,7H)-tetraone), was reacted with two electron-rich aldehyde linkers TFPB-4CHO (1,2,4,5-tetrakis(4-formylphenyl)benzene) and PyTP-4CHO (1,3,6,8-tetra(4-formylphenyl)pyrene) to yield TFPB-DNII-COF and Py-DNII-COF, respectively. These COFs featured well-defined D–A–A electronic configurations, enabling efficient photocatalytic hydrogen (H_2) evolution. Notably, Py-DNII-COF, with a narrower bandgap of 1.80 eV, exhibited superior photocatalytic performance compared to TFPB-DNII-COF, which had a larger bandgap of 2.64 eV.[36] These findings underscore the versatility of imide-based COFs in tailored photocatalytic systems, where rational donor–acceptor engineering, metal complex integration, and functional pore environments contribute to highly efficient CO_2 reduction and hydrogen evolution reactions, paving the way for clean energy generation.

5.3 Energy storage

Energy Estorage systems capture energy from various sources and store it for controlled release when required. Among these systems, rechargeable batteries and supercapacitors are widely recognized for their efficiency and applicability. The growing demand for high-performance energy storage driven by advancements in nanotechnology and the global push for clean and sustainable energy solutions has led to rapid innovation in

this sector. In particular, the adoption of rechargeable batteries such as Li-ion, Na-ion, K-ion, and Li–S batteries is accelerating, especially for powering emission-free electric vehicles and portable electronics. In rechargeable batteries, energy is stored through the reversible movement of metal ions between the anode and cathode during charge/discharge cycles. A major challenge is the development of electrode materials that combine high specific capacity and fast charge transport with long-term mechanical and chemical stability. The electrochemical performance of a battery is intrinsically linked to the structural and electronic properties of the electrode materials, which influence specific capacity, discharge rate, and cycling stability. Recently, COFs have emerged as promising materials for electrode design due to their intrinsically porous architecture, high density of redox-active sites, excellent thermal/chemical stability, and low solubility in organic electrolytes. These properties enhance ion diffusion and charge transfer, making COFs well-suited for next-generation energy storage devices. As a result, researchers have increasingly explored imide-based COFs (PI-COFs) as organic electrodes for various metal-ion batteries, including Li-ion, Na-ion, Al-ion, and aqueous dual-ion systems.

5.3.1. Li-ion batteries (LIBs). Lithium-ion batteries (LIBs) are the most mature and commercially adopted energy storage systems due to their high energy density, scalability, and recyclability. Traditional organic polymers have been explored as electrode materials in LIBs, but many suffer from poor electrochemical stability due to their high solubility in aprotic electrolytes, leading to low cyclability and poor charge transfer. To overcome these limitations, researchers have turned to imide-based COFs, which offer a more rigid framework, redox-active imide groups, and tuneable porosity. In 2018, two imide-based COFs—PIBN and PIBN-G—were synthesized by condensing tetraaminobenzoquinone (TABQ) and pyromellitic dianhydride (PMDA), with and without graphene, respectively (Fig. 5a). PIBN featured 1.5 nm pores, facilitating electrolyte diffusion and exhibiting a specific capacity of 244.8 mAh g^{-1}. Incorporation of graphene in PIBN-G enhanced electrical conductivity and lithium-ion mobility, boosting the specific capacity to 271 mAh g^{-1} (Fig. 5b).[38] In 2019, the Huang group incorporated reduced graphene oxide (rGO) into PI-COF-1 and PI-COF-2, synthesized from PMDA and amine linkers TAPA and TAPB, respectively. While the pristine COFs exhibited dense stacking, which hindered Li^+ diffusion and resulted in limited specific capacities, this issue was addressed by mechano-chemical exfoliation, yielding PI-ECOF-1 and PI-ECOF-2. At 0.1C, PI-ECOF-1 achieved 103 mAh g^{-1} experimentally, compared to a theoretical value of 142 mAh g^{-1}, and PI-ECOF-2 delivered 103 mAh g^{-1} *versus* 128 mAh g^{-1} theoretically. To bridge this performance gap, rGO was further doped into the frameworks at varying loadings (10%, 30%, and 50%), producing PI-ECOF-1/rGOX and PI-ECOF-2/rGOX (X = wt% of rGO). Notably, 30% rGO loading optimized the charge transfer and capacity retention, achieving 127 mAh g^{-1} for PI-ECOF-1/rGO (89% of its theoretical capacity) and 124 mAh g^{-1} for PI-ECOF-2/rGO (97% of theoretical capacity).[50] In addition to conductivity, porosity and surface functionalization play a critical role in determining electrode performance. To address this, a COF with dual redox-active sites (C=O and C=N) was synthesized by reacting PMDA with TAPT, forming TP-COF. Subsequent mechanical exfoliation yielded E-TP-COF with a larger pore size (~2.6 nm) and enhanced surface area. This improved the specific capacity from 25 mAh g^{-1} (TP-COF) to 110 mAh g^{-1} (E-TP-COF).[41] Using a similar approach, another dual-active-site COF, PIT-COF, was developed by reacting melamine with PMDA. It delivered an impressive specific capacity of 233 mAh g^{-1} after 300 cycles, highlighting the long-term cycling stability and robustness of imide-COF-based electrodes (Fig. 5c–e).[62] This growing body of research showcases the immense potential of imide-based COFs as next-generation electrode materials for lithium-ion batteries, combining molecular-level tunability, structural stability, and electrochemical efficiency. With further material innovation and optimization, these frameworks could significantly contribute to the development of high-performance, eco-friendly energy storage systems.

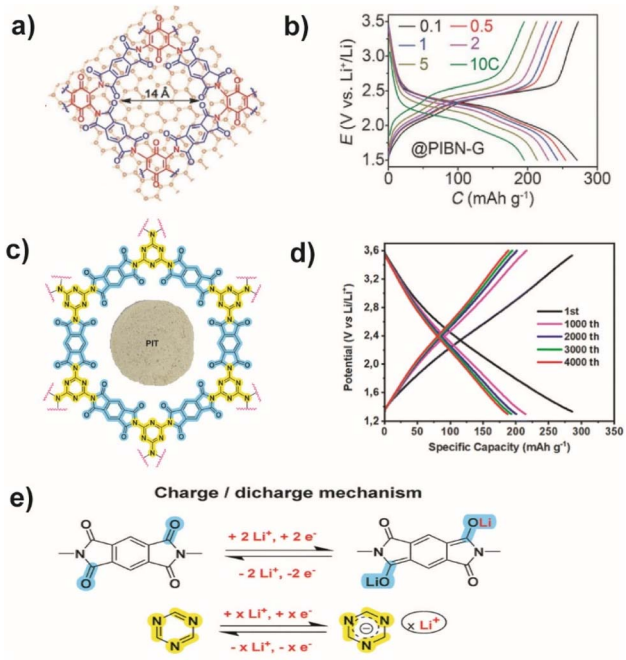

Fig. 5 (a) structural representation of PIBN-G COF. (b) Electrochemical charge/discharge curve of PIBN-G COF. (c) The structure of PIT COF, (d) electrochemical Li+ charge/discharge profile of PIT COF, (e) charge/discharge mechanism of PIT COF. Figure (a, and b) have been reproduced and adopted from reference no. 38 with permission from Wiley, copyright 2018. Figure (c, d, and e) have been reproduced and adopted from reference no. 62 with permission from RSC, copyright 2024.

5.3.2. Na-ion, Li/Na-ion, and Al-ion batteries. The commercialization of lithium-ion batteries (LIBs) in 1991 marked a pivotal moment in advancing cleaner energy storage technologies, significantly reducing dependence on fossil fuels. Despite their success, the limited availability of lithium resources and the high production costs pose serious challenges for large-scale, sustainable deployment. This has stimulated growing interest in alternative battery chemistries such

as sodium-ion (NIBs) and aluminum-ion batteries (AIBs), which utilize more earth-abundant and cost-effective materials. Imide-based COFs (PI-COFs), owing to their intrinsic redox-active carbonyl sites, high thermal/chemical stability, and tunable porosity, have emerged as promising electrode candidates for these next-generation batteries. In a recent 2024 study, two new PI-COFs HATN-PD-COF and HATN-TAB-COF were developed for sodium-ion batteries. At a current density of 200 mA g^{-1}, HATN-PD-COF demonstrated a high discharge capacity of 210 mAh g^{-1}, achieving 92% of its theoretical capacity (229 mAh g^{-1}). In contrast, HATN-TAB-COF delivered a lower capacity of 150 mAh g^{-1} (83% of theoretical 180 mAh g^{-1}), likely due to differences in structural conductivity and ion transport efficiency.[28] Simultaneously, another imide-based COF, TAPB-NDA-COF, was reported for dual lithium/sodium-ion battery applications. This COF was synthesized *via* condensation between TAPB (amine linker) and NDA (anhydride) in a 1 : 1.5 molar ratio. To enhance electronic conductivity and ion mobility, composites were formed by incorporating carbon nanotubes (CNTs) in varying loadings (10%, 30%, 50%). The optimized composite, TAPB-NDA@CNT50, exhibited excellent performance in both battery systems, with 138 mAh g^{-1} specific capacity and 81.2% retention over 2000 cycles for LIBs, and 136.7 mAh g^{-1} capacity with 80% retention over 1000 cycles for NIBs.[51] Moving beyond alkali-metal-based systems, aluminum-ion batteries (AIBs) have attracted attention due to the natural abundance and trivalent charge of Al^{3+} ions, offering high theoretical capacities. In 2023, Liu *et al.* synthesized two triazine–imide hybrid COFs 2D-PT-COF and 2D-NT-COF which served as efficient cathode materials for AIBs.[43] These frameworks uniquely incorporated p-type triazine and n-type imide moieties, enabling bifunctional redox storage: triazine units captured anionic $AlCl_4^-$, while imide moieties stored cationic $AlCl_2^+$ (Fig. 6a and b). Remarkably, 2D-NT-COF achieved a high specific capacity of 132 mAh g^{-1}, utilizing 80.5% of its redox-active sites (theoretical capacity: 152 mAh g^{-1}). In comparison, 2D-PT-COF, though having a higher theoretical capacity of 170 mAh g^{-1}, exhibited only 91 mAh g^{-1}, attributed to limited active site utilization (53.2%). These studies highlight the versatility of imide-based COFs across multiple battery systems, emphasizing their potential in building efficient, scalable, and sustainable energy storage technologies.

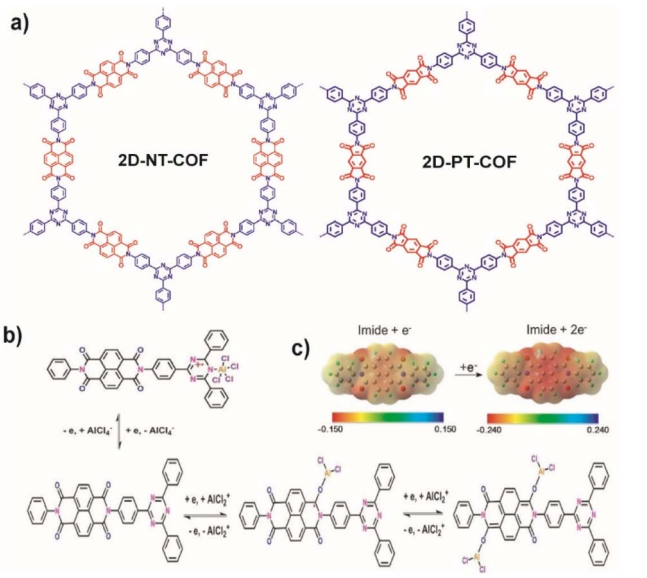

Fig. 6 a) The schematic representation of 2D-NT-COF and 2D-PT-COF. (b) Charge storage mechanism of 2D-NT-COF, (c) MESP plot of imide moiety in 2D-NT-COF. All figures have been reproduced and adopted from reference no. 43.

5.4 Adsorption and separation

5.4.1. Gas storage and separation. Imide-COFs have emerged as highly promising materials for gas adsorption and separation due to their large surface area, uniform and tunable pore structures, and exceptional chemical and thermal stability. Their well-ordered porosity enables efficient diffusion and capture of gas molecules, making them suitable for environmental remediation applications, including the adsorption of toxic gases and the separation of industrial gas mixtures. Air pollution, primarily driven by the release of hazardous gases such as SO_2, NO_2, O_3, CO_2, and particulate matter from vehicles, power plants, and industrial combustion, poses severe health and environmental risks. Among these, sulfur dioxide (SO_2), predominantly emitted by diesel-powered engines and coal-fired power plants, is a major contributor to respiratory diseases and acid rain. To address such issues, several Imide-COFs with tailored surface functionalities have been developed for the selective capture and separation of these toxic gases. In 2017, Lee Gang-Young and co-workers[52] synthesized two novel Imide-COFs using both solvothermal and microwave-assisted methods, incorporating the modulator 4-[(dimethylamino)methyl] aniline (DMMA). The DMMA units formed ionic complexes with SO_2 through electrostatic interactions, allowing the COFs to exhibit excellent SO_2 adsorption capacity with low-energy desorption, making the process both efficient and reversible. Beyond direct gas capture, Imide-COFs have also been integrated into mixed matrix membranes (MMMs) to enhance gas permeability and selectivity. In 2018, Wang and colleagues developed a MMM by incorporating MAB1-COF, synthesized from melamine and 3,3′,4,4′-biphenyl tetracarboxylic dianhydride, into a commercial P84 polyimide matrix.[49] The MMM was evaluated for N_2/O_2 separation under 0.1 MPa pressure. At 10% MAB1 loading, the membrane achieved O_2 and N_2 permeabilities of 190.37 and 290.05 Barrer, respectively, with an ideal selectivity of 1.52. When the COF loading was increased to 30%, N_2 permeability improved further to 147.02 Barrer, while O_2 permeability decreased to 76.04 Barrer, and selectivity increased to 1.93—demonstrating the tunable performance of the membrane by varying COF content. In another example, two triimide-based COFs, MTI-COF-1 and MTI-COF-2, with BET surface areas of 339 and 397 m^2 g^{-1}, respectively, were reported in 2019 for CO_2 capture.[26] These COFs exhibited CO_2 uptake capacities of 39 and 46 cm^3 g^{-1} at 273 K and 1 bar, highlighting their potential for post-combustion carbon capture. Additionally, the separation of

acetylene (C_2H_2)—a valuable yet challenging gas to isolate due to its similar physical properties to ethylene—has been successfully demonstrated using Imide-COFs. In 2018, Zhu's group developed PAF-110, an imide-based crystalline COF with a high surface area of 910 $m^2\ g^{-1}$, which exhibited preferential adsorption of C_2H_2 over C_2H_4.[39] At 273 K and 1 bar, PAF-110 captured 3.48 mmol g^{-1} of acetylene, nearly twice the uptake of ethylene (1.61 mmol g^{-1}), with a selectivity ratio of up to 3.9. This high selectivity is attributed to stronger binding interactions of acetylene with the imide-functionalized framework. These studies underscore the versatility of Imide-COFs in capturing and separating diverse gaseous species and highlight their potential role in addressing critical environmental challenges through advanced porous materials engineering.

5.4.2. Organic pollutant removal. The he exponential rise in industrialization and population density, particularly in urban regions, has led to the alarming release of toxic organic contaminants into natural water systems. Among these pollutants, synthetic dyes such as Rhodamine B (RhB) and methylene blue (MB) are of significant concern due to their non-biodegradability, carcinogenicity, and persistent ecological impact. Various physical, chemical, and biological methods have been explored for dye removal, but adsorption remains the most favorable due to its operational simplicity, low cost, high efficiency, and reusability potential.[53] Porous imide-linked PI-COFs have emerged as highly promising adsorbent materials for dye capture owing to their excellent structural tunability, chemical robustness, and large surface areas. In a landmark study in 2014, three imide-based COFs—PI-COF-1, PI-COF-2, and PI-COF-3—were reported and utilized for RhB adsorption.[12] These frameworks, synthesized *via* solvothermal methods, exhibited substantial surface areas, with PI-COF-3 demonstrating the highest BET surface area of 2346 $m^2\ g^{-1}$, outperforming PI-COF-1 (1027 $m^2\ g^{-1}$) and PI-COF-2 (1297 $m^2\ g^{-1}$). The enhanced porosity was directly correlated with increased dye uptake performance. In 2023, a new imide-COF synthesized from pyromellitic dianhydride (PMDA) and tris(4-aminophenyl) amine (TAPA) was evaluated for methylene blue removal. The COF was subjected to post-synthetic alkaline hydrolysis using various concentrations of KOH (0–5 M), which increased the surface charge and improved electrostatic interactions with the cationic MB dye.[54] At pH 10, the hydrolysed COF exhibited a maximum adsorption capacity of 315.6 mg g^{-1}, highlighting the role of electrostatic interaction in enhancing adsorption performance. More recently, Maleki *et al.* developed a hydrazone-linked imide-COF, BPM-COF, *via* condensation of PMDA and 1,3,5-tricarbohydrazide (BTCH).[55] Despite a modest surface area of only 11 $m^2\ g^{-1}$, BPM-COF demonstrated significant RhB adsorption, achieving 80.22% dye removal and a maximum capacity of 192.54 mg g^{-1} within just 6 minutes of contact time. The adsorption efficacy was attributed to multiple non-covalent interactions, including hydrogen bonding, electrostatic attractions, and van der Waals forces. This finding underscores that, apart from surface area, surface chemistry and functional group arrangement critically influence the dye adsorption behaviour of COFs.

5.5 Heavy metal sensing and removal

Heavy metal ions and radionuclides released from anthropogenic activities—such as mining, electronic waste, nuclear power generation, and pharmaceuticals—pose a severe threat to water quality and ecological safety. Elements like Fe^{3+}, Pb^{2+}, Hg^{2+}, Cu^{2+}, Cd^{2+}, and radioactive isotopes such as ^{235}U, ^{129}I, and ^{128}Pd are persistent in the environment and harmful even at trace levels due to their toxicity and bioaccumulative nature. Despite the clean energy advantages of nuclear technology, radionuclide contamination is a major concern, necessitating the development of advanced materials for efficient detection and remediation. Imide-linked COFs offer several advantages for heavy metal ion sensing and capture, including high thermal and chemical stability, uniformly distributed micropores, and electron-rich functional moieties. In 2017, two robust imide COFs—PI-COF-201 and PI-COF-202—were synthesized using a high-temperature solid-state reaction approach.[19] These frameworks displayed excellent chemical durability and potential for heavy metal adsorption, serving as a platform for future investigations. Further extending this work, Liang *et al.* utilized a PMDA-TAPB COF for the dual detection of Fe^{3+} and Pb^{2+} in aqueous systems.[56] This COF exhibited 96% fluorescence quenching for Fe^{3+} at 1 mM concentration and a limit of detection (LOD) of 1 nM for Pb^{2+} through electrochemical analysis, highlighting its high selectivity and sensitivity. In a significant recent development (2023), Run-Han *et al.* synthesized a nitrogen-rich COF, PI-COF-6, through the condensation of PMDA with 5,5′,5″-(1,3,5-triazine-2,4,6-triyl)tris(pyridin-2-amine) (TTPA).[57] The COF backbone incorporated multiple pyridine nitrogen atoms, which, in conjunction with the imide carbonyl groups, formed N–N–O tridentate binding sites for selective chelation of UO_2^{2+}. PI-COF-6 demonstrated an exceptional uranium uptake capacity of 424.5 mg g^{-1}, with 98% removal efficiency within 50 minutes. Moreover, it displayed superior selectivity over competing metal ions, showcasing the potential of structural engineering in COFs for targeted radionuclide remediation (Fig. 7).

5.6 Catalysis

Catalysts Catalysis plays a pivotal role in advancing sustainable chemistry by accelerating reaction rates, improving product selectivity, and minimizing energy consumption and waste generation. In this context, imide-linked COFs have garnered attention as highly promising heterogeneous catalysts due to their high thermal and chemical stability, permanent porosity, and the ability to incorporate active metal sites or catalytic moieties within their frameworks. A notable example is the development of Cu@PI-COF, reported by Han Yi *et al.* in 2018.[58] This catalytic system was synthesized by first constructing an imide-based COF through the solid-state condensation of melamine and pyromellitic dianhydride (PMDA), followed by post-synthetic metalation with $Cu(OAc)_2$ in ethanol at room temperature. The resulting Cu@PI-COF was evaluated as a catalyst for the Chan–Lam coupling reaction between arylboronic acids and amines. Under optimized conditions in a MeOH : H_2O (1 : 1) solvent system, the catalyst achieved a 91%

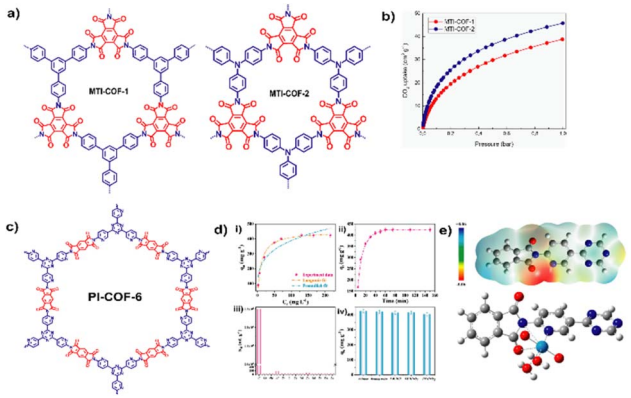

Fig. 7 (a) Structural representation of MTI-COF-1, MTI-COF-2. (b) CO_2 gas adsorption isotherm of MTI-COF-1 and MTI-COF-2, (c) the structural drawing of PI-COF-6 which have been used for uranium sequestration. (d) (i) uranium adsorption isotherm, (ii) adsorption kinetics of PI-COF-6, (iii) selectivity of PI-COF-6, (iv) adsorption stability of PI-COF-6, (e) N–N–O nano trap for Uranium in PI-COF-6. Figure (a, and b) have been reproduced and adopted from reference no. 26. Figure (c, d, and e) have been reproduced and adopted from reference no. 57 with permission from ACS, copyright 2023.

yield within 8 hours. Furthermore, it demonstrated excellent reusability, retaining catalytic performance over eight consecutive cycles with simple filtration-based recovery, underscoring its robustness and practical viability. Imide-COFs also provide an excellent platform for supporting metal nanoparticles (NPs), enabling diverse catalytic transformations. For instance, porphyrin-based imide COFs—designated PPPP-1 and PPPP-2—were synthesized solvothermally and subsequently loaded with palladium nanoparticles (Pd NPs).[59] These Pd@COFs were applied as catalysts in Suzuki–Miyaura cross-coupling reactions, a key C–C bond-forming process in pharmaceutical and fine chemical synthesis. Pd@PPPP-1 exhibited a 92% yield for the coupling of iodobenzene and phenylboronic acid after 3 hours, while Pd@PPPP-2 achieved a 94% yield for bromobenzene under similar conditions. These findings highlight the potential of tailored imide-based COFs as modular platforms for high-performance, recyclable, and green catalytic systems.

5.7 Imide COFs toward sustainable development goals (SDGs)

United Nations (UN) council has implemented 17 sustainable developmental goals (SDGs) in the year of 2015 for the betterment of the natural environment and future generation. It is interesting to note that the versatile functionality of imide-COFs aligns closely with several of the United Nations Sustainable Development Goals. More specifically imide-COFs towards clean energy and environmental remediation satisfy the well-known SDGs 6, 7 and 12.

5.7.1 SDG 6 (Clean Water and Sanitation). Water bodies near industrial zones are frequently contaminated with organic pollutants, nuclear waste, and various anthropogenic contaminants. The high surface area, tailored pore architecture, and the presence of heteroatoms such as nitrogen (N) and oxygen (O) in imide-based COFs endow them with remarkable capabilities for pollutant removal and adsorption. Imide COFs such as PI-COF-1, PI-COF-2, PI-COF-3, and BPM-COF exhibit excellent adsorption performance toward organic dyes (*e.g.*, Rhodamine B), owing to their high surface area and rich active sites.[12,55] Another variant, PI-COF, has been effectively utilized for the removal of methylene blue. Additionally, PI-COF-201, PI-COF-202, and PMDA-TAPB COFs demonstrate high selectivity and sensitivity toward Fe^{3+} and Pb^{2+} ion detection.[19,42] Of particular note, PI-COF-6 features a nano-trap architecture composed of N–N–O coordination sites, enabling the adsorption of uranyl ions (UO_2^{2+}) up to 424.5 $mg \cdot g^{-1}$ with 98% removal efficiency within 50 minutes.[57] These studies collectively highlight the exceptional potential of imide-based COFs to support SDG 6 (Clean Water and Sanitation)through efficient and sustainable wastewater treatment and pollutant remediation.

5.7.2 SDG 7 (Affordable and Clean Energy). The global transition from fossil fuels to renewable and cleaner energy sources is critical for mitigating environmental pollution and achieving low-carbon energy systems. In alignment with SDG 7 (Affordable and Clean Energy), imide-based COFs have emerged as highly promising materials for energy storage and conversion applications due to their redox-active imide linkages and tuneable electronic structures. Imide COFs such as PIC-Ph,[18] PIC-Dp,[18] HATN-AQ-COF,[27] PIBN-G,[38] TP-COF,[41] Be–PICOF,[47] Na–PICOF,[47] and Pe-PICOF,[47] PIT-COF,[62] COF-JLU-85,[63] COF-JLU-86,[63] TAPA-PDI-COF,[65] have been successfully applied in Li^+ and Zn^{2+} ion batteries, demonstrating excellent charge–discharge efficiency and cycling stability. Beyond rechargeable batteries, imide-based COFs including NDI-COF, TAPA-NDI-COF, TAPB-NDI-COF, TAPT-NDI-COF, and Cryst-2D-PMPI serve as effective electrocatalysts for key reactions such as the oxygen reduction reaction (ORR), hydrogen evolution reaction (HER), and oxygen evolution reaction (OER) in fuel cells. Moreover, their inherent porosity enables efficient CO_2 adsorption and storage, which can be further harnessed in CO_2-based photocatalytic fuel cells. Overall, these applications underline the crucial role of imide COFs in enabling the transition toward sustainable, low-emission energy systems and achieving SDG 7.

5.7.3 SDG 12 (Responsible Consumption and Production). The rapid expansion of industrial sectors such as textiles, pharmaceuticals, and fertilizers has resulted in the extensive use of diverse chemicals, many of which pose risks to human health and the environment. In this context, imide-based COFs present significant promise for promoting responsible consumption and production (SDG 12) through their multifunctional properties and green chemistry potential. The tunable pore structures and heteroatom-rich frameworks make them ideal candidates for adsorption and separation processes, enabling the selective capture of toxic gases such as SO_2, O_3, and NO_2. Imide COFs such as PMDA-TAPA,[21] PIA,[46] PIB,[46] PIC,[46] PID,[46] responsible for CO_2 adsorption, similarly MAB1 used for N_2/O_2 separation.[49] Furthermore, imide COFs have been explored as heterogeneous catalysts for environmentally benign chemical transformations, contributing to sustainable synthesis methodologies. In addition, the sensitivity of imide

COFs toward biomolecules and microbial contaminants has enabled their use as sensing materials for food safety applications helping to detect spoilage and ensure quality control in the food industry. Overall, these versatile functions underscore the potential of imide-based COFs to support sustainable industrial practices and contribute effectively toward achieving SDG 12 (Responsible Consumption and Production).

5.8 Theoretical investigations of imide COFs

In addition to experimental studies, the structures and properties of imide-based COFs have been extensively explored and rationalized through theoretical investigations. For instance, Luo *et al.*[38] reported the synthesis of an imide COF (PIBN) integrated with graphene sheets (PIBN-G) for lithium-ion battery applications. Dispersion-corrected density functional theory (DFT) calculations, performed using the Vienna *ab initio* simulation package (VASP), were employed to elucidate the interfacial interactions within the PIBN–graphene composite. Charge density difference analysis revealed pronounced charge redistribution and transfer between PIBN and graphene through π–π stacking interactions, which significantly enhanced both the structural stability and electronic conductivity of PIBN-G. More recently, in 2020, Mo and co-workers designed and constructed three COFs using TFPB as the core unit combined with different linkers namely, a cyano-substituted aromatic linker (PDAN), an anhydride linker (PMDA), and an aldehyde linker (TPAL). Among these, the cyano-functionalized COF–alkene exhibited outstanding photocatalytic hydrogen evolution (PHE) activity of 2330 μmol h^{-1} g^{-1}, outperforming both the imide- and imine-linked analogues. Complementary DFT calculations provided detailed HOMO–LUMO energy level analyses, offering valuable insights into the electronic structures responsible for the enhanced photocatalytic efficiency.[68]

6 Conclusions

In this review, we have comprehensively surveyed the current advancements in Imide-COFs, focusing on their synthetic strategies, structural properties, and emerging applications in clean energy conversion, storage, and environmental remediation. Particular emphasis has been placed on various synthetic routes, including solvothermal, microwave-assisted, ionothermal, and high-temperature solid-state methods, which enable the formation of highly crystalline and chemically robust frameworks.

The intrinsic design of imide-COFs constructed from electron-deficient aromatic dianhydrides and electron-rich aromatic amines imbues these materials with redox-active imide linkages, making them well-suited for applications such as electrocatalysis, energy storage, and gas separation. Furthermore, their high surface area, permanent porosity, and incorporation of heteroatoms enhance their performance in the adsorptive removal of organic dyes, toxic gases, and heavy metals, as well as in fluorescence-based sensing. Importantly, the versatile functionality of imide-COFs aligns closely with several of the United Nations Sustainable Development Goals (SDGs).

Remarkably, the application imide-COFs towards clean energy and environmental remediation satisfy SDGs 6, 7 and 12. Clean water and sanitation (**SDG 6**): high surface area, empirical pore architecture and the heteroatoms present in the imide-COF skeleton help to achieve great potential for the removal of organic pollutants (dyes), metals like uranium. Imide-COFs also helps in sensing of other heavy metal such as Fe^{3+}.

Affordable and clean energy (**SDG 7**): Imide-COFs are best example which can be used in batteries and fuel cells discussed in this review article. It can also be used CO_2 gas storage, which had strong potential to use as photocatalytic fuel cell in latter stage. Responsible consumption and production (**SDG 12**): Rapid industrial developments produced highly toxic chemicals, contaminants and essentially polluted the water bodies and environment which is detrimental for the human society. Imide-COFs showed good potential for the adsorption and separation of those toxic contaminants because of its tuneable pores, presence of different heteroatoms. It is used as adsorptive material for toxic gases like SO_2, O_3, NO_2, used as catalyst for the synthesis of required chemicals in a greener way.

We believe that, the significant findings of imide-COF presented in this account establish an effective class of porous architectural framework that will be useful to address the roadmap towards clean energy and sustainable environment.

Overall, these attributes position imide-COFs as an emerging class of porous organic materials with significant potential to contribute to global efforts in energy sustainability and environmental preservation. Continued exploration in framework engineering, green synthesis, and hybrid functionalization is expected to further unlock their multifunctionality and practical deployment in real-world applications.

7 Future outlook

Imide-COFs represent a rapidly emerging class of porous crystalline materials with significant promise for clean energy technologies and environmental applications, due to their exceptional thermal stability, chemical robustness, and intrinsic porosity. Despite the noteworthy progress made in recent years, the research on Imide-COFs remains in its early stages, with several critical challenges yet to be addressed to unlock their full potential. One major limitation is the restricted library of monomeric precursors, especially the limited availability of aromatic dianhydrides required for imide linkage formation. While a variety of aromatic amine-based monomers are commercially or synthetically accessible, the development of novel, highly functionalized aromatic anhydride monomers is essential. This will open avenues for the synthesis of structurally diverse and functionally tailored Imide-COFs with enhanced application-specific properties. Secondly, the synthesis methodologies employed for Imide-COFs often rely on harsh reaction conditions, including high temperatures and the use of high-boiling-point organic solvents. The field would greatly benefit from the development of greener and more sustainable synthetic approaches, such as room–temperature reactions, solvent-free or minimal solvent-assisted methods, and the use of water as a benign solvent. Additionally,

mechanochemical synthesis, which is scalable, energy-efficient, and solvent-free, presents a promising alternative for the eco-friendly bulk production of Imide-COFs. Furthermore, most reported Imide-COFs to date exhibit two-dimensional layered structures with limited topological diversity. Expanding the design space to include three-dimensional frameworks with varied topologies and interpenetration patterns could significantly improve the surface area, hierarchical porosity, and functional tunability, thereby enhancing performance in applications such as adsorption, separation, and gas storage. The introduction of hierarchical porosity—combining micro- and mesopores within a single framework—could revolutionize Imide-COF performance for size-selective pollutant capture. Smaller molecules would preferentially occupy micropores, while larger pollutants could be accommodated in meso- or macropores. This multi-scale pore engineering strategy holds enormous potential for advancing the use of Imide-COFs in wastewater treatment, gas purification, and membrane-based separations. Another important research direction is addressing the scalability and processability of Imide-COFs. Current research is primarily limited to powder forms; however, transforming these materials into processable macroscopic forms (films, pellets, monoliths) with retained crystallinity and porosity is crucial for industrial-scale applications, including 3D printing and additive manufacturing. Moreover, the redox-active imide functionalities present in these COFs make them promising candidates for energy-related applications, such as fuel cells, supercapacitors, and rechargeable batteries. The integration of transition metals (*e.g.*, Fe, Co, Pd) or the formation of polymer-COF composites could further enhance electrocatalytic activity, conductivity, and stability, facilitating their use in next-generation energy storage and conversion devices. In summary, with continuous innovation in monomer design, green synthesis, dimensionality control, and composite engineering, Imide-COFs are poised to emerge as a next-generation platform for addressing global sustainability challenges. Their tunable structure, multifunctionality, and inherent durability offer a bright future toward practical applications in energy and environmental domains, supporting long-term goals for a greener, safer, and more sustainable world.

Conflicts of interest

There are no conflicts to declare.

Data availability

No primary research results, software or code have been included, and no new data were generated or analysed as part of this review.

Acknowledgements

PP acknowledges VIT Vellore for the Assistant Professor Junior (APJ) fellowship. TP acknowledges the financial assistance of Council of Scientific & Industrial Research (CSIR, India) (sanction no: 01/3130/23 EMR-II).

Notes and references

1 K. T. Tan, S. Ghosh, Z. Wang, F. Wen, D. Rodríguez-San-Miguel, J. Feng, N. Huang, W. Wang, F. Zamora, X. Feng, A. Thomas and D. Jiang, *Nat. Rev. Methods Primers*, 2023, **3**, 1.
2 L. Tan and B. Tan, *Chem. Soc. Rev.*, 2017, **46**, 3322–3356.
3 J. X. Jiang, F. Su, A. Trewin, C. D. Wood, N. L. Campbell, H. Niu, C. Dickinson, A. Y. Ganin, M. J. Rosseinsky, Y. Z. Khimyak and A. I. Cooper, *Angew. Chem., Int. Ed.*, 2007, **46**, 8574–8578.
4 R. Dawson, A. I. Cooper and D. J. Adams, *Prog. Polym. Sci.*, 2012, **37**, 530–563.
5 A. I. Cooper, *Adv. Mater.*, 2009, **21**, 1291–1295.
6 Y. Zhang and S. N. Riduan, *Chem. Soc. Rev.*, 2012, **41**, 2083–2094.
7 Y. Zeng, R. Zou and Y. Zhao, *Adv. Mater.*, 2016, **28**, 2855–2873.
8 N. Huang, P. Wang and D. Jiang, *Nat. Rev. Mater.*, 2016, **1**, 16068.
9 A. P. Côté, A. I. Benin, N. W. Ockwig, M. O'Keeffe, A. J. Matzger and O. M. Yaghi, *Science*, 2005, **310**, 1166–1170.
10 B. J. Smith, A. C. Overholts, N. Hwang and W. R. Dichtel, *Chem. Commun.*, 2016, **52**, 3690–3693.
11 K. Geng, T. He, R. Liu, S. Dalapati, K. T. Tan, Z. Li, S. Tao, Y. Gong, Q. Jiang and D. Jiang, *Chem. Rev.*, 2020, **120**, 8814–8933.
12 Q. Fang, Z. Zhuang, S. Gu, R. B. Kaspar, J. Zheng, J. Wang, S. Qiu and Y. Yan, *Nat. Commun.*, 2014, **5**, 4503.
13 B. B. Narzary, B. C. Baker, N. Yadav, V. D'Elia and C. F. J. Faul, *Polym. Chem.*, 2021, **12**, 6494–6514.
14 Y. Zhang, Z. Huang, B. Ruan, X. Zhang, T. Jiang, N. Ma and F. Tsai, *Macromol. Rapid Commun.*, 2020, **41**, 2000402.
15 (*a*) Z. Rasheva, L. Sorochynska, S. Grishchuk and K. Friedrich, *eXPRESS Polym. Lett.*, 2015, **9**, 196–210; (*b*) C. Huang, F. Niu, G. Xie, J. Li, C. Li, Y. Wang, F. Ji, G. Zhang, R. Sun and C. Wong, *Mater. Res. Express*, 2019, **6**, 125358.
16 M. Li, B. Han, L. Gong, Y. Jin, M. Wang, X. Ding, D. Qi and J. Jiang, *Chin. Chem. Lett.*, 2024, 110590.
17 J. Lv, Y. Tan, J. Xie, R. Yang, M. Yu, S. Sun, M. Li, D. Yuan and Y. Wang, *Angew. Chem., Int. Ed.*, 2018, **57**, 12716–12720.
18 T. Kim, S. H. Joo, J. Gong, S. Choi, J. H. Min, Y. Kim, G. Lee, E. Lee, S. Park, S. K. Kwak, H. Lee and B. Kim, *Angew. Chem., Int. Ed.*, 2021, **61**, 202113780.
19 T. Wang, R. Xue, H. Chen, P. Shi, X. Lei, Y. Wei, H. Guo and W. Yang, *New J. Chem.*, 2017, **41**, 14272–14278.
20 J. Maschita, T. Banerjee, G. Savasci, F. Haase, C. Ochsenfeld and B. V. Lotsch, *Angew. Chem., Int. Ed.*, 2020, **59**, 15750–15758.
21 L. Zhao, H. Liu, Y. Du, X. Liang, W. Wang, H. Zhao and W. Li, *New J. Chem.*, 2020, **44**, 15410–15414.
22 Z. Huang, Y. Zhang, S. Zhao, Y. Xu, X. Qi, L. Zhang and Y. Zhao, *Microporous Mesoporous Mater.*, 2022, **343**, 112191.
23 C. S. Diercks and O. M. Yaghi, *Science*, 2017, **355**, eaal1585.
24 D. Tian, H.-Z. Zhang, D.-S. Zhang, Z. Chang, J. Han, X.-P. Gao and X.-H. Bu, *RSC Adv.*, 2014, **4**, 7506.

25 Q. Fang, J. Wang, S. Gu, R. B. Kaspar, Z. Zhuang, J. Zheng, H. Guo, S. Qiu and Y. Yan, *J. Am. Chem. Soc.*, 2015, **137**, 8352–8355.
26 H. Veldhuizen, A. Vasileiadis, M. Wagemaker, T. Mahon, D. P. Mainali, L. Zong, S. van der Zwaag and A. Nagai, *J. Polym. Sci., Part A:Polym. Chem.*, 2019, **57**, 2373–2377.
27 X. Yang, L. Gong, X. Liu, P. Zhang, B. Li, D. Qi, K. Wang, F. He and J. Jiang, *Angew. Chem., Int. Ed.*, 2022, **61**, e202207043.
28 X. Yang, L. Gong, Z. Liu, Q. Zhi, B. Yu, X. Chen, K. Wang, X. Li, D. Qi and J. Jiang, *Sci. China:Chem.*, 2024, **67**, 1300–1310.
29 B. Dong, W.-J. Wang, W. Pan and G.-J. Kang, *Mater. Chem. Phys.*, 2019, **226**, 244–249.
30 N. Zhao, J.-M. Liu, F.-E. Yang, S.-W. Lv, J. Wang and S. Wang, *ACS Appl. Bio Mater.*, 2021, **4**, 995–1002.
31 S. Royuela, E. Martínez-Periñán, M. P. Arrieta, J. I. Martínez, M. M. Ramos, F. Zamora, E. Lorenzo and J. L. Segura, *Chem. Commun.*, 2020, **56**, 1267–1270.
32 M. Martínez-Fernández, E. Martínez-Periñán, S. Royuela, J. I. Martínez, F. Zamora, E. Lorenzo and J. L. Segura, *Appl. Mater. Today*, 2022, **26**, 101384.
33 Z. Guo, S. Yang, M. Liu, Q. Xu and G. Zeng, *EcoEnergy*, 2024, **2**, 192–201.
34 R. Pan, J. Wu, W. Wang, C. Cheng and X. Liu, *Colloids Surf., A*, 2021, **621**, 126511.
35 X. Chen, Q. Dang, R. Sa, L. Li, L. Li, J. Bi, Z. Zhang, J. Long, Y. Yu and Z. Zou, *Chem. Sci.*, 2020, **11**, 6915–6922.
36 I. M. A. Mekhemer, M. M. Elsenety, A. M. Elewa, K. D. G. Huynh, M. M. Samy, M. G. Mohamed, D. M. Dorrah, D. C. K. Hoang, A. F. Musa, S.-W. Kuo and H.-H. Chou, *J. Mater. Chem. A*, 2024, **12**, 10790–10798.
37 C. Zhang, S. Zhang, Y. Yan, F. Xia, A. Huang and Y. Xian, *ACS Appl. Mater. Interfaces*, 2017, **9**, 13415–13421.
38 Z. Luo, L. Liu, J. Ning, K. Lei, Y. Lu, F. Li and J. Chen, *Angew. Chem.*, 2018, **130**, 9587–9590.
39 L. Jiang, Y. Tian, T. Sun, Y. Zhu, H. Ren, X. Zou, Y. Ma, K. R. Meihaus, J. R. Long and G. Zhu, *J. Am. Chem. Soc.*, 2018, **140**, 15724–15730.
40 B. Sun, X. Li, T. Feng, S. Cai, T. Chen, C. Zhu, J. Zhang, D. Wang and Y. Liu, *ACS Appl. Mater. Interfaces*, 2020, **12**, 51837–51845.
41 G. Zhao, H. Li, Z. Gao, L. Xu, Z. Mei, S. Cai, T. Liu, X. Yang, H. Guo and X. Sun, *Adv. Funct. Mater.*, 2021, **31**, 2101019–2101028.
42 X. Liang, Z. Ni, L. Zhao, B. Ge, H. Zhao and W. Li, *Microchem. J.*, 2021, **170**, 106663.
43 Y. Liu, Y. Lu, A. Hossain Khan, G. Wang, Y. Wang, A. Morag, Z. Wang, G. Chen, S. Huang, N. Chandrasekhar, D. Sabaghi, D. Li, P. Zhang, D. Ma, E. Brunner, M. Yu and X. Feng, *Angew. Chem., Int. Ed.*, 2023, **62**, e202306091.
44 M. Yu, N. Chandrasekhar, R. K. M. Raghupathy, K. H. Ly, H. Zhang, E. Dmitrieva, C. Liang, X. Lu, T. D. Kühne, H. Mirhosseini, I. M. Weidinger and X. Feng, *J. Am. Chem. Soc.*, 2020, **142**, 19570–19578.
45 P.-H. Chang, M. C. Sil, K. S. K. Reddy, C.-H. Lin and C.-M. Chen, *ACS Appl. Mater. Interfaces*, 2022, **14**, 25466–25477.
46 R. van der Jagt, A. Vasileiadis, H. Veldhuizen, P. Shao, X. Feng, S. Ganapathy, N. C. Habisreutinger, M. A. van der Veen, C. Wang, M. Wagemaker, S. van der Zwaag and A. Nagai, *Chem. Mater.*, 2021, **33**, 818–833.
47 S. Gu, X. Ma, J. Chen, R. Hao, Z. Wang, N. Qin, W. Zheng, Q. Gan, W. Luo, M. Li, Z. Li, K. Liao, H. Guo, G. Liu, K. Zhang and Z. Lu, *J. Energy Chem.*, 2022, **69**, 428–433.
48 Z. Dong, H. Pan, P. Gao, Y. Xiao, L. Fan, J. Chen and W. Wang, *Catal. Lett.*, 2022, **152**, 299–306.
49 X. Yuan, Y. Wang, G. Deng, X. Zong, C. Zhang and S. Xue, *Polym. Adv. Technol.*, 2019, **30**, 417–424.
50 Z. Wang, Y. Li, P. Liu, Q. Qi, F. Zhang, G. Lu, X. Zhao and X. Huang, *Nanoscale*, 2019, **11**, 5330–5335.
51 S. Biswas, A. Pramanik, A. Dey, S. Chattopadhyay, T. S. Pieshkov, S. Bhattacharyya, P. M. Ajayan and T. K. Maji, *Small*, 2024, **20**, 2406173.
52 G.-Y. Lee, J. Lee, H. T. Vo, S. Kim, H. Lee and T. Park, *Sci. Rep.*, 2017, **7**, 557.
53 S. Dutta, B. Gupta, S. K. Srivastava and A. K. Gupta, *Mater. Adv.*, 2021, **2**, 4497–4531.
54 Y. C Hsu, M. C. Sil, C. H Lin and C. M. Chen, *Appl. Surf. Sci.*, 2023, **612**, 155890.
55 J. Rahimi, M. T. Ijdani, H. Abbasi, M. M. Salehi and A. Maleki, *J. Hazard. Mater. Adv.*, 2025, **18**, 100680.
56 X. Liang, Z. Ni, L. Zhao, B. Ge, H. Zhao and W. Li, *Microchem. J.*, 2021, **170**, 106663.
57 R.-H. Yan, W. Jiang, W.-R. Cui, R.-P. Liang and J.-D. Qiu, *ACS Appl. Eng. Mater.*, 2023, **1**, 813–821.
58 Y. Han, M. Zhang, Y.-Q. Zhang and Z.-H. Zhang, *Green Chem.*, 2018, **20**, 4891–4900.
59 W. Zhu, X. Wang, T. Li, R. Shen, S.-J. Hao, Y. Li, Q. Wang, Z. Li and Z.-G. Gu, *Polym. Chem.*, 2018, **9**, 1430–1438.
60 X. Yang, L. Gong, Z. Liu, Q. Zhi, B. Yu, X. Chen, K. Wang, X. Li, D. Qi and J. Jiang, *Sci. China:Chem.*, 2024, **67**, 1300–1310.
61 L. Zhu, C. Zhang, R. Zhu, X. Cao, J. Bai, Y. Wang, L. Liu, H. Dong and F. Ma, *J. Hazard. Mater.*, 2024, **465**, 133320.
62 R. El Oueslati, B. Jismy, B. Flamme, N. Leclerc, F. Ghamouss and M. Abarbri, *J. Mater. Chem. A*, 2024, **12**, 15866–15873.
63 J. Li, J. Zhang, Y. Hou, J. Suo, J. Liu, H. Li, S. Qiu, V. Valtchev, Q. Fang and X. Liu, *Angew. Chem., Int. Ed.*, 2024, **63**, e202412452.
64 W. Chi, B. Liu, Y. Dong, J. Zhang, X. Sun, C. Pan, H. Zhao, Y. Ling and Y. Zhu, *Appl. Catal. B Environ. Energy*, 2024, **355**, 124077.
65 X. Liu, S. Wang, S. Liu, C. Liu, X. Li, J. Wu, D. Li, S. Xu, C. Liu and W.-Y. Lai, *Sci. China:Chem.*, 2024, **67**, 1647–1652.
66 Y. Miao, W. Jin, M. Qin, Y.-M. Shen, Y. Chen, T.-R. Wu, D.-Y. Wu, J. Xu and J. Cao, *Chem. Eng. J.*, 2024, **485**, 149986K.
67 M. W. Maegawa, V. Joseph, K. Łyczko, Y. Korol, M. J. Potrzebowski, A. Matsuda and A. Nagai, *Sci. Rep.*, 2025, **15**, 5758.
68 C. Mo, M. Yang, F. Sun, J. Jian, L. Zhong, Z. Fang, J. Feng and D. Yu, *Adv. Sci.*, 2020, **7**, 1902988.